GENETICS

Guide-free Cas9 from pathogenic *Campylobacter jejuni* bacteria causes severe damage to DNA

Chinmoy Saha[1]*, Prarthana Mohanraju[2]*, Andrew Stubbs[3], Gaurav Dugar[4†], Youri Hoogstrate[3], Gert-Jan Kremers[5], Wiggert A. van Cappellen[5], Deborah Horst-Kreft[1], Charlie Laffeber[6], Joyce H.G. Lebbink[6,7], Serena Bruens[6], Duncan Gaskin[8], Dior Beerens[1‡], Maarten Klunder[2§], Rob Joosten[2], Jeroen A. A. Demmers[9], Dik van Gent[6], Johan W. Mouton[1‖], Peter J. van der Spek[3¶], John van der Oost[2¶], Peter van Baarlen[10], Rogier Louwen[1¶]

CRISPR-Cas9 systems are enriched in human pathogenic bacteria and have been linked to cytotoxicity by an unknown mechanism. Here, we show that upon infection of human cells, *Campylobacter jejuni* secretes its Cas9 (CjeCas9) nuclease into their cytoplasm. Next, a native nuclear localization signal enables CjeCas9 nuclear entry, where it catalyzes metal-dependent nonspecific DNA cleavage leading to cell death. Compared to CjeCas9, native Cas9 of *Streptococcus pyogenes* (SpyCas9) is more suitable for guide-dependent editing. However, in human cells, native SpyCas9 may still cause some DNA damage, most likely because of its ssDNA cleavage activity. This side effect can be completely prevented by saturation of SpyCas9 with an appropriate guide RNA, which is only partially effective for CjeCas9. We conclude that CjeCas9 plays an active role in attacking human cells rather than in viral defense. Moreover, these unique catalytic features may therefore make CjeCas9 less suitable for genome editing applications.

INTRODUCTION

CRISPR-Cas is an RNA-guided adaptive defense system that enables prokaryotes to recognize and destroy the nucleic acids of invading genetic elements (i.e., viruses or plasmids) by Cas nucleases (*1*). Besides providing adaptive immunity, CRISPR-Cas systems have been demonstrated to play a role in other processes (*2*), including bacterial pathogenicity (*3*). Comparative genomic analysis demonstrated high prevalence of type II CRISPR-Cas systems, characterized by the presence of the *Cas9* gene, in bacterial pathogens (*4*). In the pathogens, such as *Francisella novicida*, *Neisseria meningitidis*, and *Campylobacter jejuni*, Cas9 activity was found to correlate with the death of infected human cells (*5*, *6*) or infected laboratory animals (*6*).

The Cas9-encoding operons in strains of *C. jejuni* typically contain small or degenerated CRISPR arrays (fig. S1A) (*7*), which play only a minor role, at most, in viral defense (*5*). One of the proposed roles for type II CRISPR-Cas system in pathogenicity is the Cas9-mediated silencing of the expression of genes encoding exposed cell wall lipoproteins through an antisense mechanism; infectious bacteria have effectively used this strategy to evade the human immune system (*8*). Another important phenomenon is the capacity of several intracellular bacterial pathogens that harbor Cas9, including *C. jejuni*, to induce double-strand DNA breaks (DSBs) in infected human host cells, either actively by secreted bacterial cytotoxins or passively by activating the host's cell death responses (*9*). Multiple cytotoxins have been identified in *C. jejuni*, such as the cytolethal distending toxin (CDT), a bacterial toxin that induces host DNA damage (*10*). However, CDT lacking *C. jejuni* isolates still induce DNA damage (*11*), and campylobacteriosis (*12*, *13*) indicated that an additional factor is involved in the induction of DNA damage and eukaryotic cell death. Previously, we reported on the role of CRISPR-Cas9 system in *C. jejuni* virulence and disease severity and revealed that damage induced upon human cells in cellular infection assays correlated with the presence of *C. jejuni* Cas9 (CjeCas9) (*5*); others have reported that *cas9* was differentially expressed during *C. jejuni* passage across the mouse intestine (*14*). However, the molecular mechanism responsible for the observed *CjCas9*-related cytotoxicity remained elusive (*5*). Here, we show that upon the release of the CjeCas9 nuclease, *C. jejuni* induces DNA damage that leads to human cell death.

RESULTS AND DISCUSSION

CjeCas9 is secreted via OMVs into human cells

First, to validate our previous work (*5*), we corroborated by complementation a role for CjeCas9 in cytotoxicity (fig. S1, B and C). We then explored how *C. jejuni* releases the 984–amino acid protein CjeCas9 to unleash its toxic effect on human cells. Some studies support the notion that cytotoxins are secreted either by dedicated export systems (*9*) or by outer membrane vesicles (OMVs) (*15*). The pathogenic *C. jejuni* reference isolate NCTC11168 produces OMVs (*15*, *16*) that contain CjeCas9, as identified by a proteomic

[1]Department of Medical Microbiology and Infectious Diseases, Erasmus MC, University Medical Center Rotterdam, Rotterdam, Netherlands. [2]Laboratory of Microbiology, Wageningen University, Wageningen, Netherlands. [3]Clinical Bioinformatics, Department of Pathology, Erasmus MC, University Medical Center Rotterdam, Rotterdam, Netherlands. [4]Institute of Molecular Infection Biology (IMIB)/Research Center for Infectious Diseases (ZINF), University of Würzburg, Würzburg, Germany. [5]Optical Imaging Center, Erasmus MC, University Medical Center Rotterdam, Rotterdam, Netherlands. [6]Department of Molecular Genetics, Erasmus MC, University Medical Center Rotterdam, Rotterdam, Netherlands. [7]Department of Radiation Oncology, Erasmus MC, University Medical Center Rotterdam, Rotterdam, Netherlands. [8]Institute of Food Research, Gut Health and Food Safety Programme, Norwich Research Park, Norwich, UK. [9]Proteomics Center, Erasmus MC, University Medical Center Rotterdam, Rotterdam, Netherlands. [10]Host-Microbe Interactomics Group, University of Wageningen, Wageningen, Netherlands.
*These authors contributed equally to this work.
†Present address: Swammerdam Institute for Life Sciences, University of Amsterdam, Amsterdam, Netherlands.
‡Present address: Max Planck Unit for the Science of Pathogens, Berlin, Germany.
§Present address: Department of Molecular Genetics, Erasmus MC, University Medical Center Rotterdam, Rotterdam, Netherlands.
‖Deceased.
¶Corresponding author. Email: r.louwen@erasmusmc.nl (R.L.); p.vanderspek@erasmusmc.nl (P.J.v.d.S.); john.vanderoost@wur.nl (J.v.d.O.)

analyses (*16*). We therefore investigated whether CjeCas9 is present in the OMVs of our *C. jejuni* model strain GB11, a strain genetically highly similar to the isolate NCTC11168 (*17*). First, we made a CjeCas9-mCherry variant in our model strain by fusing the *cas9* gene to the *mCherry* gene from which a red fluorescent protein is produced to track CjeCas9 in human cells after being released from the *C. jejuni* OMVs. Subsequently, after isolation of the OMVs, produced and secreted by our model strain and the reference isolate NCTC11168, CjeCas9 or CjeCas9-mCherry were both detected on a Western blot containing the OMV lysates (fig. S2A). We then performed bacterial infection experiments to study the release of CjeCas9-mCherry by *C. jejuni* into human cells. By fluorescence microscopy, we observed that CjeCas9-mCherry accumulated in the cytoplasm and the nucleus (Fig. 1A and fig. S2B). As *C. jejuni* infections of human cells are accompanied by severe DNA damage (*18*), we speculated that the observed nuclear localization and the nuclease activity of CjeCas9 (*19*) could play a direct role in the pathogenicity of *C. jejuni* (fig. S2, C and D), including the induction of DNA damage (fig. S2E).

CjeCas9 nuclear entrance of human cells is facilitated by an autonomous nuclear localization signal

The observed nuclear localization of native CjeCas9, produced by *C. jejuni* bacteria during their infection of human cells, indicated that CjeCas9 was able to enter the nuclei of human cells without prior addition of a synthetic nuclear localization sequence (NLS). To assay for the autonomous nuclear entry of CjeCas9, we fused the genes that code for CjeCas9 and enhanced green fluorescent protein (eGFP) into a eukaryotic expression vector. After the transfection of the recombinant expression vectors into human cells, we observed nuclear eGFP-CjeCas9 accumulation by fluorescence microscopy (Fig. 1B and fig. S3A) and a Western blot analysis (Fig. 1C). In silico analysis of the GB11 CjeCas9 protein sequence predicted a potential NLS in the Cas9 arginine-rich bridging helix (BH) (*20*) region (fig. S3B), which plays an important role in guide RNA binding (*21*). The predicted NLS in CjeCas9 shares extensive sequence identity with arginine-rich domain sequences that occur in the viral dual-function proteins that enable RNA binding and nuclear localization (*22*, *23*). To assess whether the predicted CjeCas9 NLS facilitated nuclear entry, the DNA fragment encoding the CjeCas9 NLS region was fused to the *egfp* gene in the same eukaryotic expression vector, as described above. After the transfection of human cells, correctly expressed eGFP-NLS (CjeCas9) accumulated in the nucleus, almost as efficiently as eGFP fused to the well-established NLS of Simian virus (SV) 40 large T antigen protein (fig. S3C). Deletion of the NLS region in CjeCas9 disabled its accumulation into the nucleus (fig. S3D), validating the relevance of the NLS region for the nuclear entry of CjeCas9.

CjeCas9 induces DNA damage in human cells

The observed nuclear localization, together with the established endonuclease activity of CjeCas9 (*19*), led us to hypothesize that CjeCas9 produced and released by *C. jejuni* during infection of human cells could potentially alter DNA integrity and cell homeostasis. This idea originated from two studies that revealed that Cas9-mediated DSBs induced a p53-mediated DNA damage response in human cells, a phenomenon that may also lead to cell death (*24*, *25*). We used antibody staining to investigate whether the p53-binding protein 1 (53BP1), an important regulator of the cellular response during DSB repair (*26*), is activated in human cells upon infection with *C. jejuni* bacteria. Six hours after infection, the microscopic analysis revealed significantly increased numbers of 53BP1 foci in the nuclei of human cells that were infected with either Cas9-producing wild-type (WT) GB11 or a complemented GB11Δ*cas9*::*cas9* (Δ*cas9*::*cas9*) *C. jejuni*

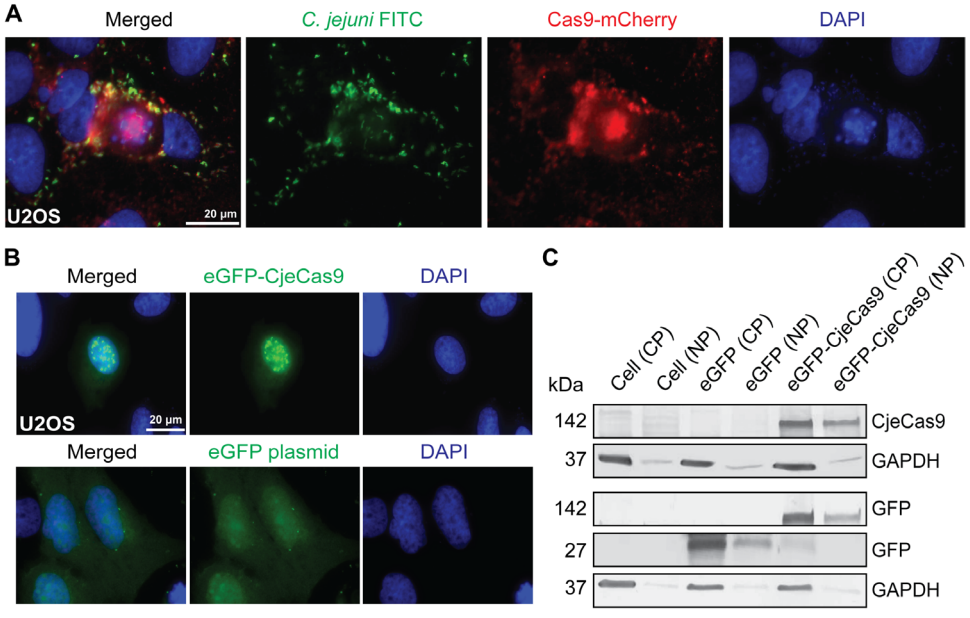

Fig. 1. CjeCas9 is released by *C. jejuni* during infection of human cells and translocate into their nuclei. (**A**) Representative microscopic images of human cells infected with *C. jejuni* bacteria (anti–*C. jejuni* FITC, green) expressing Cas9-mCherry (red). FITC is fluorescein isothiocyanate, a green fluorescent tracer. (**B**) Representative microscopic images of nuclear eGFP (enhanced green fluorescent protein)–CjeCas9 localization in human cells (green). The eGFP transfected cells represent a control. (A and B) Nuclei are counterstained with 4′,6-diamidino-2-phenylindole (DAPI) (blue). (**C**) Nuclear (NP) and cytoplasmic (CP) protein fractions of human cells. Glyceraldehyde phosphate dehydrogenase (GAPDH) verified the quality of the separation.

bacteria but not in the cells infected with the corresponding *cas9* deletion mutant, GB11Δ*cas9* (Δ*cas9*) (Fig. 2, A and B). This observation was validated in infection assays similar to those above but now by using the phosphorylated histone H2A variant X (γ-H2AX), a well-established histological marker of DSB-associated chromatin decondensation (*27*). Upon infection by CjeCas9-producing bacteria (WT or Δ*cas9*::*cas9*) (Fig. 2, C and D, and fig. S4, A to C) or exposure to the OMVs produced by these bacteria (fig. S4, D and E), human cells displayed bright red nuclei after fluorescent antibody staining of γ-H2AX. Compared to human cells infected with CjeCas9-producing bacteria, significantly fewer γ-H2AX–positive bright red nuclei or activated 53BP1-positive foci were observed in human cells infected with the Δ*cas9* bacteria (Fig. 2, A to D, and fig. S4, A, C, and F) or when exposed to their OMVs (fig. S4, D and E). Although infection efficiencies of *C. jejuni* isolates may differ substantially (fig. S4G) (*5*), the significantly reduced activation of 53BP1 and γ-H2AX in human cells challenged with Δ*cas9* bacteria cannot be simply explained by their lower infection efficiency. We observed a factor 1000 increase in invasion numbers for GB11 compared to NCTC11168 bacteria, whereas the overall CjeCas9-induced cytotoxicity (*5*) and DNA damage, as measured by 53BP1 and γ-H2AX, was equal (Fig. 2, A to D, and fig. S4, A and C to F). Together, this suggests that the cytotoxicity of *C. jejuni* strains may not be substantially influenced by adhesion and invasion but more by the secretion of differential CjeCas9 variants (*5*, *7*), the relative abundances of Cas9 in OMVs, the amounts of OMVs secreted by a strain, and the amounts of human cells that are targeted by OMVs released by the corresponding strain.

Comparative genomics indicated that *C. jejuni* strains produce varying numbers of virulence factors (*28*, *29*). However, to date, only CDT has been shown to damage DNA (*9*). CjeCas9 is a nuclease that cleaves double-stranded DNA (dsDNA) (*19*, *30*), but its potential role to induce DNA damage during infection has not yet been studied. To discriminate between the activities of CDT and Cas9, infection studies as described above were performed using two *C. jejuni* strains that both expressed CjeCas9 but produced or lacked CDT. By analyzing the DNA integrity and cell homeostasis as above, it was revealed that human cells infected with either producing or nonproducing CDT *C. jejuni* bacteria, of which the latter also lacked *cas1*, *cas2*, and CRISPR RNAs (crRNAs), displayed the same degree of activation of

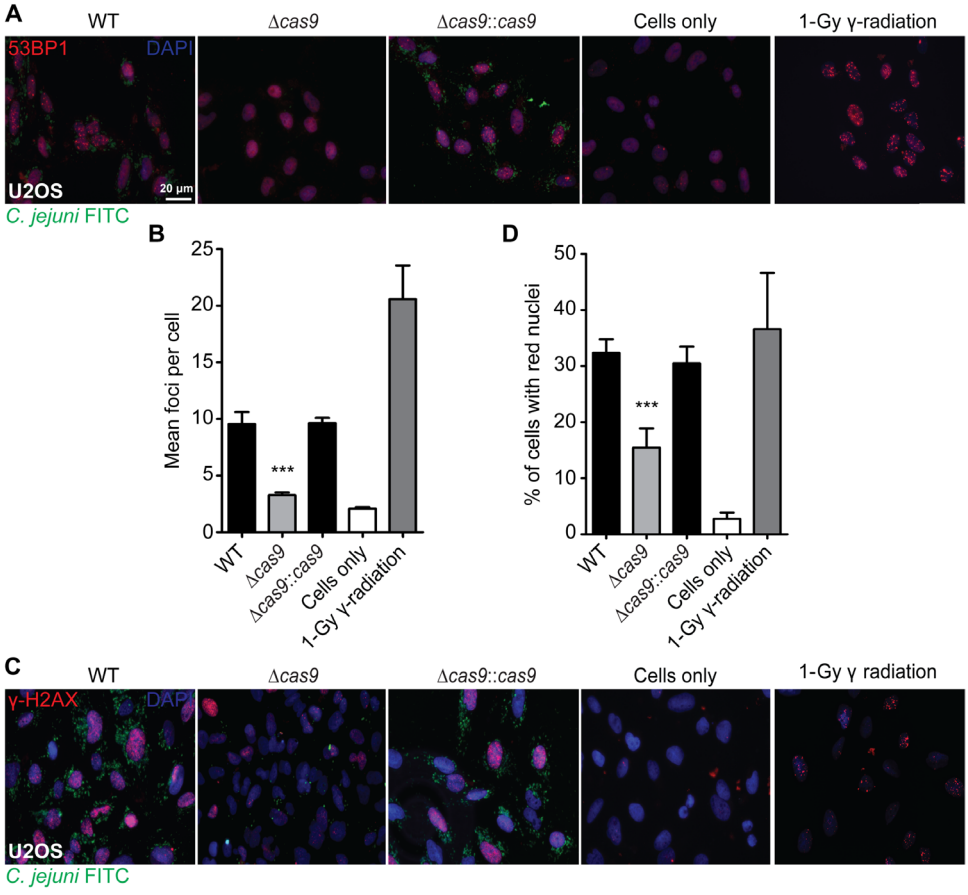

Fig. 2. CjeCas9 activates the chromatin and DNA integrity markers, 53BP1 and γ-H2AX, in U2OS cells. *C. jejuni* GB11 (WT) and its variants Δ*cas9* or Δ*cas9*::*cas9* were stained with anti–*C. jejuni* FITC (green), and nuclei were counterstained with DAPI (blue). Gamma (γ)–irradiated cells are used as a positive control, and untreated cells were used as a negative control. (**A**) Representative microscopic images of human cells infected with WT, Δ*cas9*, or Δ*cas9*::*cas9* were stained for 53BP1 (red). (**B**) The number of 53BP1 related foci per cell (mean foci per cell, *y* axis) were counted in human cells. The *C. jejuni* bacteria used are shown on the *x* axis. (**C**) Representative microscopic images of human cells infected with WT, Δ*cas9*, or Δ*cas9*::*cas9* were stained for γ-H2AX (red). (**D**) The percentage of human cells with bright red nuclei is displayed on the *y* axis. The *C. jejuni* bacteria used are listed at the *x* axis. Values represent means ± SEM. ***$P < 0.001$ [one-way analysis of variance (ANOVA), Bonferroni's multiple comparison test].

γ-H2AX and 53BP1 (fig. S5, A to C). These results corroborated previous studies, demonstrating that CDT is not the sole factor responsible for disrupting chromatin and DNA integrity during human cell infection by *C. jejuni* (*11*, *31*).

To examine whether, specifically, the CjeCas9 nuclease activity leads to disruptions in human cellular chromatin and DNA integrity, we quantified γ-H2AX–stained nuclei in human cells that were transduced with plasmids encoding either eGFP-CjeCas9 or its catalytically inactive (dead) variant, eGFP-CjedCas9 [introduction of a single-nucleotide polymorphism (SNP) in *cjecas9* could be more accurately controlled and validated in plasmids than in the *C. jejuni* genome]. At comparable transfection efficiencies (fig. S6, A and B), significantly elevated frequencies of γ-H2AX–positive nuclei were detected in human cells transfected with eGFP-CjeCas9 as compared to cells transfected with eGFP-CjedCas9 (fig. S6C). These results were further validated by Western blot analysis of γ-H2AX in lysates generated from transfected eukaryotic cells (fig. S6D). The 53BP1, γ-H2AX immunohistochemistry, and γ-H2AX Western blotting results thus support the notion that CjeCas9 catalytic nuclease activity alters human chromatin and DNA integrity.

CjeCas9 is associated with the induction of DSBs

The BLESS (direct in situ breaks labelling, enrichment on streptavidin and next-generation sequencing) method (*32*) was used during infection experiments with Cas9-producing and nonproducing strains to obtain a genome-wide snapshot impression profile of DNA DSB induction correlating with CjeCas9 activity. The BLESS analysis (Fig. 3A) revealed that human cells infected for 6 hours with WT or Δ*cas9*::*cas9* bacteria harbored substantial numbers of DSBs (Fig. 3B, and fig. S7, A and B), of which 678,910 (WT) or 942,104 (Δ*cas9*::*cas9*) were CjeCas9 dependent (table S1). Note that numbers of unique Cas9-dependent DSBs were obtained after background correction, i.e., subtraction of DSBs obtained by BLESS from uninfected (93,373) or Δ*cas9* bacteria–infected (190,111) human cells incubated in parallel (table S1). The BLESS data thus showed that production of native CjeCas9 correlated with increased numbers of DSBs in nuclei of infected human cells (Fig. 3B and fig. S7, A to D), consistent with our data on 53BP1 and γ-H2AX activation. The three reported CjeCas9 protospacer adjacent motifs (PAMs) (*19*, *33*, *34*) were not enriched adjacent to the detected DSBs (Fig. 3C and table S2), indicating that the processing of human cellular DNA by native CjeCas9 during infection by *C. jejuni* is PAM independent.

RNA-independent genomic DNA cleavage by CjeCas9

Our finding that CjeCas9 could be cleaving PAM independently is in line with a recent analyses describing that Cas9 proteins obtained from *Streptococcus pyogenes* (SpyCas9) and *F. novicida* (FnoCas9) cleave plasmid DNA in a PAM- and RNA-independent manner (*35*). In the absence of a guide RNA, SpyCas9 (type II-A) cleaves single-stranded DNA (ssDNA), while FnoCas9 (type II-B) nicks plasmid dsDNA (*35*). These RNA-independent activities are dependent on Mg^{2+}/Mn^{2+} cations and require the RuvC domain of SpyCas9 and the HNH domain of FnoCas9 (*35*). We considered that these metal ions most likely play an important role in the PAM- and RNA-independent DNA processing activity of CjeCas9. Plasmid cleavage experiments in the presence of Mg^{2+} using purified recombinant

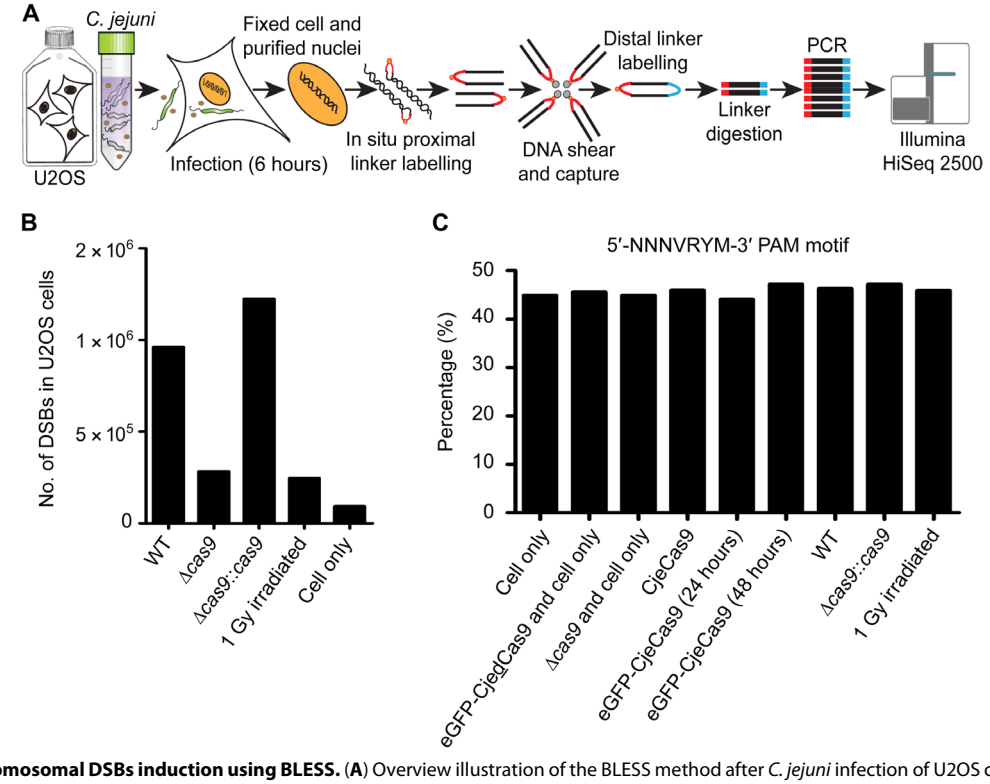

Fig. 3. Analysis of chromosomal DSBs induction using BLESS. (**A**) Overview illustration of the BLESS method after *C. jejuni* infection of U2OS cells. (**B**) Histogram showing numbers of DSBs accumulated during bacterial infection. Cells that were 1 Gy (gray) irradiated are used as a positive control. Untreated cells were used as a control in the BLESS analyses. (**C**) Example outcome of PAM analyses. *y* axis shows the percentage of the 5′-NNNVRYM-3′ PAM motif that is detected in the BLESS-obtained DSBs breaks, as observed in raw and filtered datasets obtained from the samples shown on the *x* axis.

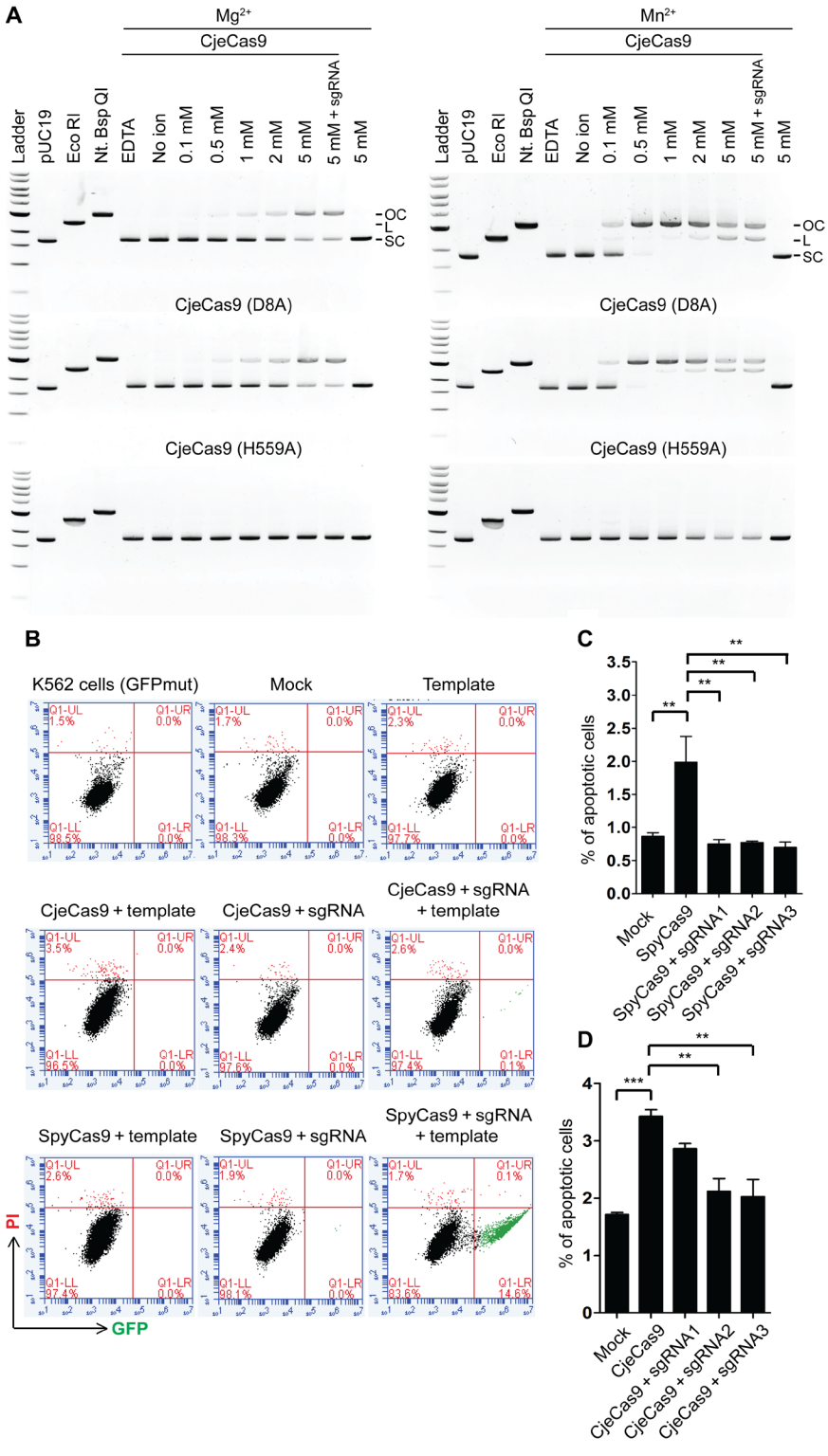

Fig. 4. In vitro cleavage assay and in vivo genome editing efficiencies of native CjeCas9 and SpyCas9 in human cells. (**A**) CjeCas9 activity and the effect of divalent cations (Mn^{2+} and Mg^{2+}) concentration on plasmid DNA cleavage. SC is super coiled, L is linear, and OC is open-circle plasmid DNA. (**B**) Restoration of GFP expression mediated by CjeCas9 or SpyCas9 genome editing in human cells [K562(GFPmut)] and quantified using FACS. In Q1-LR, the percentages of CjeCas9 or SpyCas9 genome edited cells that have a restored GFP expression are visualized (green). Q1-UL are dead cells. Q1-UR are GFP-positive dead cells. Q1-LL are unedited [K562(GFPmut)] cells. (**C** and **D**) Percentages of apoptotic human cells (K562) obtained after 6 hours. Concentration of CjeCas9 or SpyCas9 is 30 pmol, and for the sgRNA, the concentrations are 30, 60, and 90 pmol [for single guide RNA1 (sgRNA1), sgRNA2, and sgRNA3, respectively]. Results shown as means ± SEM. ***$P < 0.001$ and **$P < 0.01$ (one-way ANOVA, Bonferroni's multiple comparison test).

CjeCas9 and SpyCas9 proteins (fig. S8A) showed that activity of these nucleases was Mg^{2+} dependent (fig. S8B). Guide-free CjeCas9-induced DSBs in the presence of at least 2 mM Mn^{2+} or nicks at 500 μM Mg^{2+} or 100 μM Mn^{2+} in plasmid dsDNA (Fig. 4A). Notably, *C. jejuni* infects mainly the intestinal epithelial cells of the jejunum (*36*), where the highest concentrations of the divalent cations manganese and magnesium can be found. Physiological ranges for turnover of manganese are in an adult 0.9 to 10 mg/day (*37*), for magnesium this is about 300 mg/day (*38*); the jejunum also adsorbs 125 mM/day magnesium (*39*). Noteworthy, manganese is crucial for pathogens to colonize and attack the host, with specific systems being activated to fight for this crucial metal ion uptake (*40*). The tested Mn^{2+} and Mg^{2+} metal ion concentrations used in the in vitro CjeCas9 assays are thus of biological relevance. Under the same experimental conditions, SpyCas9 did not cleave dsDNA (fig. S9A), but it did cleave ssDNA (fig. S9B), reproducing findings from a different study (*35*). To identify whether the divalent cation-dependent cleavage of plasmid dsDNA by CjeCas9 was catalyzed by the RuvC or HNH domain, we carried out the same metal ion–dependent cleavage assays with WT, as well as RuvC and/or HNH active site mutants of CjeCas9. We found that the guide-independent activity of CjeCas9 that cleaves plasmid dsDNA was completely abolished in both the HNH-inactive single mutant and the HNH/RuvC-inactive double mutant (Fig. 4A and fig. 9C). This shows that the guide-independent processing of double-stranded plasmid DNA depends on the activity of the CjeCas9 HNH domain in the presence of Mn^{2+} or Mg^{2+}. When CjeCas9 or its active site–mutated variants were incubated together with human chromosomal DNA isolated from U2OS cells, CjeCas9 with a functional HNH domain and Mn^{2+} or Mg^{2+} cations were sufficient to completely degrade human genomic DNA (fig. S10, A and B), confirming the results obtained with the plasmid DNA. This finding was validated by staining for γ-H2AX on a Western blot containing eukaryotic cell lysates generated from human cells transfected with eukaryotic expression vectors that enabled the expression of CjeCas9, CjeCas9ΔRuvC, CjeCas9ΔHNH, or the dead variant CjedCas9 (fig. S10C).

The RNA guide-independent processing of double-stranded human DNA by CjeCas9 that we observed is very different from the reported guide-dependent targeting activity by SpyCas9, the most frequently used enzyme in genome editing applications (*41*). We tested the extent to which the features observed for CjeCas9 also apply to SpyCas9. First, we fused eGFP to full-length SpyCas9 or its arginine-rich BH motif and cloned them into a eukaryotic expression vector, after which the two different vectors were transfected into human cells. Fluorescence microscopy (fig. S11, A and B) and Western blot analysis of the cytoplasmic and nuclear fractions (fig. S11C) revealed that eGFP-SpyCas9 does not require an exogenously introduced NLS to reach the nucleus. Next, GFP-SpyCas9 activated γ-H2AX, indicating that DNA integrity had been altered (fig. S12, A and B), as observed for GFP-CjeCas9. In vitro incubations of chromosomal DNA and SpyCas9 indicated that SpyCas9 does not cleave dsDNA (fig. S12C), whereas CjeCas9 does (fig. S10B). However, in human cells, guide-free SpyCas9 alters DNA integrity as measured by γ-H2AX activation (fig. S12D). This likely relates to the guide-free activity of SpyCas9 targeting ssDNA on transiently exposed regions of the chromosomes (fig. S9B).

Comparing genome editing efficiencies between native CjeCas9 and SpyCas9

We then used an established procedure to compare genome editing efficiencies of native CjeCas9 and SpyCas9 in human cells. Briefly, native Cas9 proteins together with a *gfp*-targeting RNA guide and a homologous *gfp*-repair template were introduced by lipofection into human cells to restore a mutated *gfp* gene in the genomic AAVS1 locus; successful editing events result in restored GFP production that can be quantified by fluorescence-activated cell sorting (FACS) analysis (*42*). We found that genome editing by CjeCas9 was at least 100 times less efficient than by SpyCas9 (Fig. 4B and fig. S13, A to D), which, in part, may be because of the poor helicase activity of this enzyme (*43*). We noticed differences in the number of dead cells when comparing guide-free Cas9 nucleases with Cas9 nucleases saturated with a guide RNA during genome editing procedures. Dedicated analyses using SpyCas9 and CjeCas9 revealed that saturation of native SpyCas9 proteins with a nontargeting guide RNA reduced numbers of death cells to background levels (Fig. 4C), whereas saturation of CjeCas9 proteins with a nontargeting guide RNA only slightly reduced the numbers of dead cells (Fig. 4D). This difference could relate to the reduced binding strength of guide RNAs to the relatively small CjeCas9 protein (*43*).

In conclusion, we demonstrate here that Cas9 proteins can autonomously translocate into the nucleus of human cells. In here, Mn^{2+}- or Mg^{2+}-dependent DNA processing by guide-free Cas9 proteins occurs nonspecifically, and dsDNA nicking and DSB induction activities of CjeCas9 may lead to substantial genomic DNA damage that may overwhelm human cells and prohibit their survival. Metal ion–dependent and RNA-independent CjeCas9 activity provides a clear mechanistic explanation for the cytotoxicity to human cells we previously observed in *C. jejuni* infection experiments using human cells (*5*). We propose a working model on the role of CjeCas9 in bacterial-induced cytotoxicity (fig. S14). Overall, we conclude that CjeCas9 has the potential to actively participate in the attack of human cells rather than in the defense against viruses. Moreover, the unique catalytic features of CjeCas9 may therefore make this nuclease less suitable for genome editing applications.

MATERIALS AND METHODS

Bacterial strains and growth conditions

The *C. jejuni* isolates used in this work harbor a type II-C CRISPR-Cas system, but GB11 lacks a CRISPR array (*5*, *17*) and the *C. jejuni* (*cdt*-) strain only harbors *cas9* (fig. S1A). All the used strains are listed together with their generated *cas9* variants in table S3. The methods for generating Δ*cas9* and growth conditions have been described previously (*5*). The same method was used for generating the Δ*cas9*::*cas9* as for generating Δ*cas9* (*5*), with the exception that not *cas9* was disrupted but *Cj0046c* in the Δ*cas9* mutant. This pseudogene was replaced by homologous recombination with a promoter-driven *cjecas9* gene and an appropriate antibiotic gene for selection. WT and the genetic variant strains were cultured on blood agar plates containing 7% sheep blood (Becton Dickinson, Breda, The Netherlands) and the appropriate antibiotics (Sigma-Aldrich, Zwijndrecht, The Netherlands) for mutant and complemented mutant selection (table S3). Cultures were performed under microaerophilic conditions at 37° using anaerobic jars and an Anoxomat (Mart Microbiology B.V., Drachten, The Netherlands). Infection experiments occurred at a multiplicity of infection (MOI) of 100 bacteria per one host cell, unless stated otherwise.

Maintenance of human cell lines

Human intestinal epithelial cell line Caco-2 (human epithelial colorectal adenocarcinoma cells), HeLa cells (human cervical cancer

cells), U2OS cells (human osteosarcoma cells), K562 (chronic myelogenous leukemia), and HEK293T cells (human embryonic kidney cells) were maintained in Dulbecco's modified Eagle's medium (DMEM) [Thermo Fisher Scientific (TFS), Bleiswijk, The Netherlands] supplemented with 10% fetal bovine serum (FBS) (TFS, Bleiswijk, The Netherlands), penicillin (100 U/ml) (TFS, Bleiswijk, The Netherlands), streptomycin (100 μg/ml) (TFS, Bleiswijk, The Netherlands), and 1% nonessential amino acids (NEAA) (TFS, Bleiswijk, The Netherlands). The human cells were cultured in a 75-cm^2 flask (Greiner Bio-One, Alphen aan den Rijn, The Netherlands) at 37°C and 5% CO_2 in a humidified air incubator (Binder, Tuttlingen, Germany). All experiments were performed with the U2OS cell line unless stated otherwise. For example, HEK293T cells were used for technical reasons in experiments requiring a cancer cell line that adheres more loosely for more efficient cytoplasmic and nuclear fraction separations. To study the cell death induction, K562 suspension cells were used to prevent stress exposure by the trypsin/EDTA procedure that could affect the results obtained by the FACS analyses. All cell lines were ordered from the American Type Culture Collection for human cell lines and were routinely tested for mycoplasma.

Adhesion and invasion

The adherence and invasion of *C. jejuni* was determined by growing the U2OS cells to confluence at a final approximate density of 5.0×10^6 cells per well (Greiner Bio-One, Alphen aan den Rijn, The Netherlands). The adherence and invasion assays were performed by incubating the epithelial cells with *C. jejuni* at a ratio of 1:100. Bacteria and epithelial cells were coincubated for 20 min at 37°C under a 5% CO_2 and 95% air atmosphere to assess adherence. For invasion, a subsequent 2-hour incubation of the epithelial cells was allowed. After incubation, monolayers were washed three times with prewarmed Hank's balanced salt solution (HBSS) (TFS, Bleiswijk, The Netherlands). To sacrifice extracellular bacteria, monolayers were treated for 3 hours with a bactericidal concentration of gentamicin (480 μg/ml; Sigma-Aldrich, Zwijndrecht, The Netherlands) in DMEM (TFS) containing 10% FBS (TFS) and 1% NEAA (TFS). After a wash, epithelial cells were lysed with 0.1% Triton X-100 (Cornell, Philadelphia, PA) in HBSS (TFS) for 15 min at room temperature. The number of *C. jejuni* bacteria that had invaded the cells was determined by plating serial dilutions of the lysis mix onto freshly prepared blood agar plates. After incubation for 24 to 36 hours at 37°C in a microaerobic environment, colonies were counted and the colony-forming units per milliliter (CFU/ml) was calculated. For determination of adherence, cells were washed extensively three times with HBSS (TFS) after 15 to 20 min of incubation with the *C. jejuni* isolates. This time slot was sufficient to study adherence as reported (*44*). The cell monolayer was then detached with 0.1% Triton X-100 (Sigma-Aldrich), after which serial dilutions were plated onto Columbia blood agar plates (Becton Dickinson, Breda, The Netherlands). After incubation for 24 to 36 hours at 37°C in a microaerobic environment, colonies were counted, and the CFU/ml was calculated.

Cell death assay

Cells were seeded on six-well plates (Greiner Bio-One, Alphen aan den Rijn, The Netherlands) at a density of 1.0×10^5 cells per well and allowed to form a monolayer (U2OS, Caco-2, and HeLa cells). When the cells reached confluence, the medium was replaced with the maintenance medium without antibiotics. U2OS, Caco-2, HeLa, and K562 cells were infected at an MOI of 100 with WT, Δ*cas9*, or Δ*cas9*::*cas9* bacteria. Here, the infection process was followed over time using a phase contrast fluorescence microscope. At 24 to 120 hours after infection, pictures were taken to visualize deformation, detachment, and cell debris indicating cell stress or death. For the FACS analyses to assess apoptosis induction, K562 suspension cells were infected with WT, Δ*cas9*, and the Δ*cas9*::*cas9* bacteria. Samples were collected at different time intervals (3 to 24 hours). Cells were then harvested for flow cytometry analysis (BD Accuri C6, BD Biosciences). To quantify the presence of dead cells, propidium iodide (PI; Sigma-Aldrich, Zwijndrecht, The Netherlands) staining was used according to the manufacturer's protocol.

Isolation of *C. jejuni* OMVs

C. jejuni OMVs were isolated as described previously (*16*, *31*). Briefly, overnight, *C. jejuni* cultures were centrifuged at 5000*g* for 30 min, and the resulting supernatant was filtered across a 0.22-μm membrane (Corning, New York, USA). The filtrate was concentrated to 13 ml using an iCON Concentrator (TFS, Bleiswijk, The Netherlands) 20 ml/9 K. The concentrated filtrate was ultracentrifuged at 150,000*g* for 3 hours at 4°C using a SW 41 Ti Rotor (Beckman Coulter, Woerden, The Netherlands). All isolation steps were carried out at 4°C. The pellet was resuspended in phosphate-buffered saline (PBS) (TFS, Bleiswijk, The Netherlands) and stored at −80°C. OMV samples were pipetted onto blood agar plates containing 7% sheep blood (Becton Dickinson, Breda, The Netherlands) and incubated under both microaerophilic and (an)aerobic conditions for 48 hours to confirm the absence of viable bacteria. OMVs were quantified using the EVQuant (*45*).

Generation of *C. jejuni* bacteria expressing Cas9-mCherry fusion proteins

The *C. jejuni* Cas9-mCherry strains (table S3) were generated by overlap extension polymerase chain reaction (PCR) as described previously (*46*). Briefly, the primers that were used to amplify *cas9*-introduced overlapping ends for the *mCherry* gene (table S4). By using this overlap PCR method, we generated a single PCR product combining the individual PCR fragments for Cas9 and mCherry and a kanamycin resistance gene to allow for antibiotic selection. Then, the single Cas9-mCherry PCR product generated was introduced into the native *cas9* locus of *C. jejuni* by electroporation to generate an mCherry-tagged Cas9 strain through homologous recombination.

In silico Cas9 protein sequence motif analyses

The Cas9 protein sequences from *S. pyogenes* M1-GAS (AAK33936.1), *Staphylococcus aureus* subsp. *aureus* (CCK74173.1), *Listeria monocytogenes* SLCC2482 (CBY05127.1), *Francisella tularensis* subsp. *novicida* U112 (ABK89648.1), *N. meningitidis* 8013 (C9X1G5.1), *Helicobacter cinaedi* ATCCBAA-847 (YP_007601284.1), *Campylobacter lari* CF89-12 (BAK69486.1), *C. jejuni* NCTC11168 (YP_002344900.1), and *C. jejuni* GB11 (*5*) were uploaded into the online MyHits motif scan software tool (http://myhits.isb-sib.ch/cgi-bin/motif_scan). The NLS motifs obtained were aligned using MUSCLE (www.ebi.ac.uk/Tools/msa/muscle/), and the alignments were visualized and evaluated to identify amino acids with similar biochemical characteristics using MEGA6 software (*47*).

Creation of expression clones for Cas9 proteins and NLS motifs

The coding sequences of the Cas9 proteins of *C. jejuni* and *S. pyogenes* or their NLS motifs were cloned into the pEGFP-C1 (Clontech,

Saint-Germain-en-Laye, France) vector for coexpression in eukaryotic cells. The pCDNA 3.1(+) vector (Invitrogen, Breda, The Netherlands) was used to express native *C. jejuni* or *S. pyogenes* Cas9 proteins in eukaryotic cells. The *spycas9* or its catalytically inactive ("dead") variant, *spydcas9* gene, was cloned from the plasmids pMJ806 and pMJ841. These plasmids were provided by J. Doudna, University of California (UC) Berkeley, USA (*30*). Primers and plasmids used in this study are listed in tables S4 and S5, respectively. The presence of the CRISPR array and *cas* and *cdt* genes were analyzed by PCR using previously described methods (*5*, *44*, *48*). Genomic DNA were isolated using a QIAamp DNA tissue stool kit (QIAGEN, Venlo, The Netherlands), and PCR amplification was performed using a Biomed Thermal Cycler System 9700 (TFS, Bleiswijk, The Netherlands). DNA digestion with restriction enzymes (New England Biolabs, Leiden, The Netherlands), ligation with a T4 DNA ligase (TFS, Bleiswijk, The Netherlands), purification, and agarose gel electrophoresis were performed according to the manufacturer's protocols. Primer pairs and corresponding restriction enzymes used in this study are listed in table S4. The resulting constructs were electroporated at 2.5 kV, 200 ohm, and 25 μF into *Escherichia coli* TOP10 cells (TFS, Bleiswijk, The Netherlands), resuspended in 37°C prewarmed super optimal broth with catabolite repression medium (TFS, Bleiswijk, The Netherlands), and allowed to recover with gentle shaking at 37°C. After recovery, 100 μl was plated onto a lysogeny broth (LB) (Becton Dickinson, Breda, The Netherlands) agar plate containing the appropriate selection marker (table S5). Positive colonies were cultured for plasmid DNA isolation (TFS, Bleiswijk, The Netherlands), and plasmids were sequenced using a BigDye Terminator sequencing kit (TFS, Bleiswijk, The Netherlands) and an ABI PRISM 3100 Genetic Analyzer (TFS, Bleiswijk, The Netherlands), according to the manufacturer's instructions.

Cas9 mutagenesis

A PCR-based site-directed mutagenesis method (*46*) was used to generate a catalytically inactive (dead) Cas9 (mutated D8A and H559A) or a ΔNLS (BH) variant in CjeCas9 that was cloned into the pEGFP-C1 vector to obtain a GFP in-frame fusion protein at the C-terminal end of CjCas9. Primers are listed in table S4. Plasmids were transformed into chemically competent *E. coli* TOP10 cells (TFS, Bleiswijk, The Netherlands). After plasmid multiplication and isolation, the presence of the correct genetic mutations was confirmed by DNA sequencing.

Plasmid transfection

Human cells were seeded onto a two-well chamber slide (Sanbio, Uden, The Netherlands) at a density of 5.0×10^4 cells/ml. The next day, cells were transiently transfected with plasmid DNA using X-tremeGENE DNA Transfection Reagent (Roche Applied Science, Woerden, The Netherlands), according to the manufacturer's protocols. After incubating at 37°C and 5% CO_2 in a humidified incubator (Binder, Tuttlingen, Germany), the human cells were washed with prewarmed HBSS (TFS, Bleiswijk, The Netherlands) and fixed with 4% paraformaldehyde (Sigma-Aldrich, Zwijndrecht, The Netherlands) for immunocytochemistry and microscopy, as described previously (*44*).

SDS-PAGE and Western blot analysis

C. jejuni bacteria or their OMVs were analyzed for the presence of CjeCas9 and CjeCas9-mCherry using SDS–polyacrylamide gel electrophoresis (SDS-PAGE) gel followed by Western blotting and staining with a *C. jejuni* anti-Cas9 antibody (*5*). Plasmid-transfected cells were washed with HBSS (TFS, Bleiswijk, The Netherlands), and cell lysates were prepared by adding Bond-Breaker TCEP solution (TFS, Bleiswijk, The Netherlands) in 2× Laemmli sample buffer (Bio-Rad, Veenendaal, The Netherlands) (1:9) before loading on a SDS-PAGE gel. Cellular lysates were then denatured at 95°C for 5 min and immediately run through 4 to 20% Mini-PROTEAN TGX Precast Protein Gels (Bio-Rad, Veenendaal, The Netherlands). After electrophoresis, the proteins were blotted onto a polyvinylidene difluoride nitrocellulose membrane (Millipore, Amsterdam, The Netherlands). The membranes were blocked with PBS (TFS, Bleiswijk, The Netherlands) containing 5% nonfat dry milk (Bio-Rad, Veenendaal, The Netherlands) for 2 to 3 hours at room temperature or overnight at 4°C. For the detection of CjeCas9, SpyCas9, or their GFP-Cas9 fusion proteins, the membranes were incubated with primary polyclonal antibodies against CjeCas9 (*5*), monoclonal mouse anti-SpyCas9 (Abcam, Cambridge, UK), or rabbit polyclonal anti-GFP (NB600-308, Novus Biologicals, Abingdon, UK) at a dilution of 1:1000 and incubated for 1.5 to 2 hours at room temperature. Appropriate secondary antibodies with alkaline phosphatase (Sigma-Aldrich, Zwijndrecht, The Netherlands) were used at a dilution of 1:1000 to visualize the primary antibody binding using nitro blue tetrazolium/bromochloroindolyl phosphate (NBT/BCIP) solution (Sigma-Aldrich, Zwijndrecht, The Netherlands) according to the manufacturer's instructions. For cytoplasmic and nuclear protein fractions, NE-PER Nuclear and Cytoplasmic Extraction Reagents (TFS, Bleiswijk, The Netherlands) were used, and proteins from eukaryotic cells were extracted according to the manufacturer's instructions. Cytoplasmic and nuclear proteins were separated in a 4 to 20% Mini-PROTEAN TGX Precast Protein Gel (Bio-Rad, Veenendaal, The Netherlands). These were then Western blotted and incubated with one of the following: primary Cas9 antibodies, a mouse monoclonal anti–phospho-histone H2A.X (Ser139) clone JBW301 (Millipore, Amsterdam, The Netherlands) at a 1:1000 dilution, or a mouse monoclonal anti–glyceraldehyde phosphate dehydrogenase (GAPDH) antibody (Abcam, Cambridge, UK) at a dilution of 1:5000. These steps were taken to detect the presence of Cas9 and the presence of DNA DSBs or to control for fraction quality and equal loading. Visualization was achieved with a NBT/BCIP solution (Sigma-Aldrich, Zwijndrecht, The Netherlands) according to the manufacturer's instructions. Quantification of the Western blot data occurred with the ImageJ software (*49*) using the analyzed gel option followed by surface plotting to analyze the pixel distribution on the Western blot. During these analyses, the background was set as white, and GAPDH, a house-keeping gene, was used as a loading control.

In vitro infection assays using glass chamber slides for microscopy

Cells were seeded onto two-well chamber slides (Greiner Bio-One, Alphen aan den Rijn) at a density of 1.5×10^5 cells per well and incubated overnight at 37°C with 5% CO_2 in a humidified incubator (Binder, Tuttlingen, Germany). Cells were exposed to NCTC11168, GB11, their derived genetic variants, or *C. jejuni* bacteria lacking CDT (*cdt*-). After overnight incubation at 37°C with 5% CO_2 in a humidified air incubator (Binder, Tuttlingen, Germany), human cells were washed three times with prewarmed HBSS (TFS) at 37°C and fixed with 4% paraformaldehyde (Sigma-Aldrich, Zwijndrecht, The Netherlands). Fixed cells were prepared for γ-H2AX or 53BP1

immunocytochemistry (see below) and/or (fluorescence) microscopy analyses, as described earlier (*44*).

Immunocytochemistry

For immunofluorescence detection, plasmid-transfected human cells were washed and fixed with 4% paraformaldehyde before permeabilization with 0.1% Triton X-100 (Sigma-Aldrich, Zwijndrecht, The Netherlands). For γ-H2AX or 53BP1 antibody detection, human cells were incubated with a mouse anti–γ-H2AX antibody (Millipore, Amsterdam, The Netherlands) or rabbit polyclonal anti-53BP1 (NB100-304, Novus Biologicals, Abingdon, UK) at a 1:1000 dilution. Secondary labeling and slide preparation were conducted as described previously (*44*). To visualize *C. jejuni* in human cells, an anti–*C. jejuni* fluorescein isothiocyanate–labeled antibody (Genway, San Diego, USA) was used. The nuclei of the eukaryotic cells were counterstained with 4′,6-diamidino-2-phenylindole (DAPI). Labeling, detection of intracellular *C. jejuni* bacteria, and slide preparation were performed as previously described (*44*). Images were taken using a XI51 phase-contrast fluorescence microscope (Olympus, Leiden, The Netherlands) and further analyzed using Olympus cellSens or ImageJ/Fiji software (*49*). For 53BP1, more than 100 cells were analyzed in which the numbers of red 53BP1 foci per cell were counted. Then, the mean number of foci per cell was calculated per image taken by dividing the number of foci by the total number of human cells detected in the microscopic field. When we tested for the presence of γ-H2AX, more than 100 cells were analyzed for the presence of bright red nuclei. For Δ*cas9* exposed cells, even more independent bright red foci were included as bright red nuclei and were enumerated. The percentage of bright red nuclei was calculated by counting the number of cells with bright red nuclei (based on our own criteria) and dividing them by the total number of cells in the same microscopic field, including cells without bright red nuclei, and then multiplying by 100.

Generation of heterologous plasmids for Cas9 protein expression

For heterologous expression, the NCTC11168 *cjeCas9* gene from the pEC-K-CBP-NTAP plasmid (donated by M. Jinek, University of Zurich, Switzerland) and the *spyCas9* gene from the pET-28b-Cas9-His plasmid [obtained from A. Schier (Addgene plasmid no. 47327]) were PCR-amplified using Q5 DNA polymerase (New England Biolabs, Leiden, The Netherlands). We encountered serious technological difficulties when trying to express CjeCas9 of strain GB11 in *E. coli*. Therefore, we expressed CjeCas9 of *C. jejuni* strain NCTC11168 in *E. coli*. The amplified genes were inserted into the plasmid pML-1B (obtained from the UC Berkeley MacroLab, Addgene no. 29653) or pET28b backbone by NEBuilder HiFi DNA Assembly (New England Biolabs, Leiden, The Netherlands) using the oligonucleotides shown in table S4. This was done to generate a protein expression construct encoding the SpyCas9 or CjeCas9 polypeptide sequence fused with a C-terminal (for SpyCas9) and an N-terminal tag (for CjeCas9) comprising a hexahistidine sequence and a tobacco etch virus (TEV) protease cleavage site. The assembly mix was used to transform the competent *E. coli* DH5α strain (New England Biolabs, Leiden, The Netherlands). The plasmids were isolated and verified by Sanger sequencing (Macrogen, Amsterdam, The Netherlands) before transforming the *E. coli* Rosetta 2 (DE3) strain. The plasmids containing the WT genes were used as PCR templates to generate active site mutants of SpyCas9 and CjeCas9 via site-directed mutagenesis. In SpyCas9, D10A, H840A, and D10A-H840A amino acid substitutions yielded a RuvC, HNH, and double mutant, respectively. In NCTC11168 CjeCas9, D8A, H559A, and D8A-H559A amino acid substitutions yielded a RuvC, HNH, and double mutant, respectively. All bacterial expression plasmids used in this study can be found in table S5.

Cas9 expression and purification

Purification protocols were adapted from previously established Cas12a purification methods (*50*). The NCTC11168 *cjecas9* and *spycas9* genes were heterologous expressed in *E. coli* and purified using a combination of Ni^{2+} affinity, cation exchange, and gel filtration chromatography steps. Three liters of LB growth medium with ampicillin (100 μg/ml) were inoculated with 30 ml of overnight culture of Rosetta cells (DE3) (EMD Millipore, Ontario, Canada) containing the expression constructs. Cultures were grown to an optical density at 600 nm (OD_{600nm}) of 0.5 to 0.6. Expression was induced by adding isopropyl β-D-1-thiogalactopyranoside to a final concentration of 0.2 mM, and incubation was continued overnight at 18°C. Cells were harvested by centrifugation, and the cell pellet was resuspended in 50 ml of lysis buffer [20 mM tris-HCl (pH 8), 500 mM NaCl, and 5 mM imidazole supplemented with protease inhibitors (Roche, Woerden, The Netherlands)]. Cells were lysed by sonication, and the lysates were centrifuged for 45 min at 4°C at 30,000*g* to remove insoluble material. The cleared lysate was applied to a 5-ml HisTrap HP column (GE Healthcare, Eindhoven, The Netherlands). The column was washed with 10 column volumes of wash buffer [20 mM tris-HCl (pH 8), 250 mM NaCl, and 20 mM imidazole], and the bound proteins were eluted in elution buffer [20 mM tris-HCl (pH 8), 250 mM NaCl, and 250 mM imidazole]. Fractions containing pure proteins were pooled, and TEV protease was added in a 1:100 (w/w) ratio. The sample was dialyzed against a dialysis buffer [20 mM Hepes-KOH (pH 7.5) and 250 mM KCl] at 4°C overnight. For further purification, the protein was diluted 1:1 with 10 mM Hepes-KOH (pH 7.5) and loaded on a HisTrap Heparin HP column (GE Healthcare, Eindhoven, The Netherlands). The column was washed with ion exchange chromatography (IEX) buffer A [20 mM Hepes-KOH (pH 7.5) and 150 mM KCl] and eluted with IEX buffer B [20 mM Hepes-KOH (pH 7.5) and 2 M KCl] by applying a gradient from 0 to 50% over a total volume of 60 ml. Peak fractions were analyzed by SDS-PAGE, and fractions containing the Cas9 protein were combined. Then, dithiothreitol (DTT; Sigma-Aldrich, Zwijndrecht, The Netherlands) was added to a final concentration of 1 mM. The protein was fractionated on a HiLoad 16/600 Superdex 200 gel filtration column (GE Healthcare, Eindhoven, The Netherlands) and eluted with size exclusion chromatography (SEC) buffer [20 mM Hepes-KOH (pH 7.5), 500 mM KCl, and 1 mM DTT). Peak fractions were combined, concentrated to 10 mg/ml, flash frozen in liquid nitrogen, and either used directly for biochemical assays or stored frozen at −80°C for future use.

GFP expression and FACS analysis

For genome editing and FACS analyses, we used the K562(GFPmut) cell line (*42*), which was seeded into a 24-well plate (Greiner Bio-One, Alphen aan den Rijn, The Netherlands). Cells were then recovered overnight at 37°C at 5% CO_2 in a humidified air incubator (Binder, Tuttlingen, Germany). We then transfected the K562(GFPmut) cells (TFS, Bleiswijk, The Netherlands) with a CRISPR ribonucleoprotein (RNP) complex consisting of bacterial NCTC11168 CjeCas9 or

SpyCas9 (New England Biolabs, Leiden, The Netherlands) and a synthetic guide RNA (Biolegio, Nijmegen, The Netherlands) using Lipofectamine 2000 (TFS, Bleiswijk, the Netherlands). In addition, a PCR product generated from the GFP gene was transfected at the same time. Production of active RNP complexes and lipofection were carried out according to the manufacturer's protocols. The synthetic guide RNA sequence for SpyCas9 (gRNA_AAVS1-T2) was described earlier (*42*), and the guide for CjeCas9 single guide RNA is listed in table S5. Seventy-two hours after transfection, the K562(GFPmut) cells were harvested using ice-cold HBSS (TFS, Bleiswijk, The Netherlands) and kept on ice. After the second wash, the cells were resuspended in 0.4 ml of HBSS (TFS) containing PI from an apoptosis detection kit (GeneCopoeia, Rockville, USA). After 20 min, the K562(GFPmut) cells were analyzed using FACS (BD Accuri C6) and BD Accuri C6 Software (version 8.8.6).

DNA DSB detection using BLESS

U2OS cells were seeded into 75-cm^2 flasks (±1 to 5 million cells) (Greiner Bio-One, Bleiswijk, The Netherlands) and allowed to grow to confluence at 37°C at 5% CO_2 in a humidified air incubator (Binder, Tuttlingen, Germany). Cells were infected with GB11, GB11Δ*cas9*, or GB11Δ*cas9*::*cas9* bacteria in a humidified air incubator (Binder, Tuttlingen, Germany) at 37°C and 5% CO_2. After 6 hours, samples were fixed and prepared for sequencing according to the BLESS protocol (*32*) to obtain a snapshot of induced DSBs. This procedure was repeated for plasmid-transfected cells, which were harvested and processed for sequencing after 24 or 48 hours, respectively. As a positive control for DSB induction, a U2OS cell line harboring a stably integrated genomic I–Sce I restriction site was used according to the original BLESS protocol (*32*). In addition, gamma (γ) irradiation was applied for random induction of DSBs. U2OS cells received 1 gray (Gy) of ^{137}Cs γ radiation at a dose rate of 0.6 Gy min^{-1}. After irradiation, cells were allowed to recover for 30 min at 37°C with 5% CO_2 in a humidified air incubator (Binder, Tuttlingen, Germany) and further processed according to the original BLESS protocol. Paired-end sequencing of samples with Illumina HiSeq2500 v4 was performed by an accredited service provider (ServiceXS, Leiden, The Netherlands), according to the manufacturer's protocol (Illumina). The resulting FASTQ files were demultiplexed, and 75–base pair–sized genomic sequence fragments including the BLESS primers (*32*) and sequencing barcodes were removed. The resulting FASTQ files were mapped as paired reads per sample using Burrows-Wheeler Alignment Maximal Exact Matches (BWA MEM) (version 0.7.12.1) against the GRCh37/hg19 human genome assembly. Duplicate reads were flagged using Picard MarkDuplicates (version 1.136.0), and high-quality duplicate reads with a mapping quality score of >30 were selected using SAMtools (version 1.19). The forward read from these sequences, including genomic location, were stored as ASCII files. The frequency of reads at the same genomic location was determined for each sample, and only those positions for which four reads or more were mapped to DSBs were selected for further analysis. The frequency results from the experimental control sample were used to filter nonspecific DSBs from all other test samples based on genomic location. Reads associated with positive DSBs were visualized using the Integrated Genome Viewer (version 2.3), and a summary of the breakpoint comparisons was visualized as circos plots generated using the R (version 3.1.1) circlize package (https://cran.r-project.org/web/packages/circlize/index.html, version 0.3.8).

PAM motif identification

The identified DSB positions on the GRCh37/hg19 genome obtained by BLESS were used to extract nucleotides upstream and downstream of DSB positions using the Fetch software tool and the extract genomic DNA feature using coordinates from assembled/unassembled genomes that are available in Galaxy version 2.2.4 (http://usegalaxy.org). The extracted sequences, 10 bases upstream or downstream of the cleavage site obtained from the raw and filtered BLESS datasets, were analyzed from 5′ to 3′ and from 3′ to 5′ for the presence of a potential PAM motif. This was accomplished using WebLogo (http://weblogo.berkeley.edu/logo.cgi) or manually in Excel (Microsoft) using frequency counting of the nucleotides A, T, C, G at each individual position upstream or downstream of the break position using text filter options. This was done because the BLESS technique can sometimes result in the filling or removal of overhanging nucleotides at the DSB position that can then change the potential PAM position (*32*). The extracted sequences were further analyzed.

In vitro Cas9 U2OS genomic DNA digestion assays

Genomic DNA cleavage assays were performed in a final volume of 30 μl with 300 ng of DNA isolated from the U2OS cell line. DNA was isolated from cultured cells using a DNeasy blood and tissue kit (QIAGEN, Venlo, The Netherlands), then treated with ribonuclease A (Promega Benelux B.V., Leiden, The Netherlands), and purified. A total of 30 pmol of NCTC11168 CjeCas9 and SpyCas9 proteins (final concentration of 1 μM) were used for cleavage reaction with or without different metal ions (Mg^{2+}/Mn^{2+}) in the cleavage buffer [20 mM Hepes (pH 7.5), 150 mM KCl, 0.5 mM DTT, and 0.1 mM EDTA) and incubated at 37°C for 1, 6, and 24 hours. Different restriction enzymes (New England Biolabs, Leiden, The Netherlands) were used with their appropriate buffer as controls. The reactions were stopped by adding proteinase K and 6× DNA loading dye, purple (New England Biolabs, Leiden, The Netherlands). The genomic DNA was resolved on an agarose gel (0.8%) or denaturing urea-agarose gel (1%) stained with SYBR Gold Nucleic Acid Gel Stain (TFS, Bleiswijk, The Netherlands) and visualized using a Amersham Typhoon Gel and Blot Imaging Systems (GE Healthcare, Eindhoven, The Netherlands). To denature genomic DNA, the reactions were stopped at indicated time points by adding 40 μl of denaturing sample buffer containing 8 M urea and 0.3% SDS. Samples were denatured by incubating them for 10 min at 85°C and loading them directly on a 1% urea (2 M) agarose gel in tris-acetate-EDTA buffer as described (*51*).

Plasmid cleavage assay

Plasmid cleavage assays were performed in a final volume of 20 μl with 6 nM plasmid DNA (pUC19) and 100 nM CjeCas9 (NCTC11168) or SpyCas9 nucleases in the presence of 10 mM EDTA or 5 mM either $MgCl_2$ or $MnCl_2$ at 37°C for 1 hour. Other metal salts were tested but did not show any activation of the CjeCas9 (NCTC11168) or SpyCas9 nucleases. As a control, the reaction was performed without any added metal or EDTA to account for any fortuitous metal associated with the protein preparation. The reactions were stopped by adding 10 mM EDTA and 1% SDS, after which 6× DNA loading dye (New England Biolabs, Leiden, The Netherlands) was added. The DNA was resolved on an agarose gel (0.8%) stained with SYBR Safe DNA Gel Stain (TFS, Bleiswijk, The Netherlands) and visualized using a G:BOX F3 gel imager (Syngene, Bangalore, India). To create DNA mobility standards, pUC19 was separately treated with a linearizing enzyme Eco RI (New England Biolabs, Leiden,

The Netherlands) or the nicking enzyme Nt. Bsp QI (New England Biolabs, Leiden, The Netherlands). Both Eco RI and Nt. Bsp QI have a single recognition site in the pUC19 plasmid.

SUPPLEMENTARY MATERIALS

Supplementary material for this article is available at http://advances.sciencemag.org/cgi/content/full/6/25/eaaz4849/DC1

View/request a protocol for this paper from *Bio-protocol*.

REFERENCES AND NOTES

1. P. Mohanraju, K. S. Makarova, B. Zetsche, F. Zhang, E. V. Koonin, J. van der Oost, Diverse evolutionary roots and mechanistic variations of the CRISPR-Cas systems. *Science* **353**, aad5147 (2016).
2. E. R. Westra, A. Buckling, P. C. Fineran, CRISPR-Cas systems: Beyond adaptive immunity. *Nat. Rev. Microbiol.* **12**, 317–326 (2014).
3. R. Louwen, R. H. J. Staals, H. P. Endtz, P. van Baarlen, J. van der Oost, The role of CRISPR-Cas systems in virulence of pathogenic bacteria. *Microbiol. Mol. Biol. Rev.* **78**, 74 (2014).
4. D. H. Haft, J. Selengut, E. F. Mongodin, K. E. Nelson, A guild of 45 CRISPR-associated (Cas) protein families and multiple CRISPR-Cas subtypes exist in prokaryotic genomes. *PLoS Comput. Biol.* **1**, e60 (2005).
5. R. Louwen, D. Horst-Kreft, A. G. Boer, L. Graaf, G. Knegt, M. Hamersma, A. P. Heikema, A. R. Timms, B. C. Jacobs, J. A. Wagenaar, H. P. Endtz, J. Oost, J. M. Wells, E. E. S. Nieuwenhuis, A. H. M. Vliet, P. T. J. Willemsen, P. Baarlen, A. Belkum, A novel link between *Campylobacter jejuni* bacteriophage defence, virulence and Guillain–Barré syndrome. *Eur. J. Clin. Microbiol. Infect. Dis.* **32**, 207–226 (2013).
6. T. R. Sampson, S. D. Saroj, A. C. Llewellyn, Y.-L. Tzeng, D. S. Weiss, A CRISPR-Cas system mediates bacterial innate immune evasion and virulence. *Nature* **497**, 254–257 (2013).
7. B. M. Pearson, R. Louwen, P. van Baarlen, A. H. M. van Vliet, Differential distribution of Type II CRISPR-Cas systems in agricultural and nonagricultural *Campylobacter coli* and *Campylobacter jejuni* isolates correlates with lack of shared environments. *Genome Biol. Evol.* **7**, 2663–2679 (2015).
8. H. K. Ratner, A. s. Escalera-Maurer, A. s. L. Rhun, S. Jaggavarapu, J. E. Wozniak, E. K. Crispell, E. Charpentier, D. S. Weiss, Catalytically active Cas9 mediates transcriptional interference to facilitate bacterial virulence. *Mol. Cell* **75**, 498–510.e5 (2019).
9. C. Chumduri, R. K. Gurumurthy, R. Zietlow, T. F. Meyer, Subversion of host genome integrity by bacterial pathogens. *Nat. Rev. Mol. Cell Biol.* **17**, 659–673 (2016).
10. M. Lara-Tejero, J. E. Galán, A bacterial toxin that controls cell cycle progression as a deoxyribonuclease I-like protein. *Science* **290**, 354–357 (2000).
11. L. D. Kalischuk, G. D. Inglis, A. G. Buret, Strain-dependent induction of epithelial cell oncosis by *Campylobacter jejuni* is correlated with invasion ability and is independent of cytolethal distending toxin. *Microbiology* **153**, 2952–2963 (2007).
12. N. P. Mortensen, P. Schiellerup, N. Boisen, B. M. Klein, H. Locht, M. Abuoun, D. Newell, K. A. Krogfelt, The role of *Campylobacter jejuni* cytolethal distending toxin in gastroenteritis: Toxin detection, antibody production, and clinical outcome. *APMIS* **119**, 626–634 (2011).
13. H. Nielsen, S. Persson, K. E. P. Olsen, T. Ejlertsen, B. Kristensen, H. C. Schønheyder, Bacteraemia with *Campylobacter jejuni*: No association with the virulence genes *iam*, *cdtB*, *capA* or *virB*. *Eur. J. Clin. Microbiol. Infect. Dis.* **29**, 357–358 (2010).
14. J. P. Jerome, J. A. Bell, A. E. Plovanich-Jones, J. E. Barrick, C. T. Brown, L. S. Mansfield, Standing genetic variation in contingency loci drives the rapid adaptation of *Campylobacter jejuni* to a novel host. *PLOS ONE* **6**, e16399 (2011).
15. C. Schwechheimer, M. J. Kuehn, Outer-membrane vesicles from Gram-negative bacteria: Biogenesis and functions. *Nat. Rev. Microbiol.* **13**, 605–619 (2015).
16. K.-S. Jang, M. J. Sweredoski, R. L. J. Graham, S. Hess, W. M. Clemons, Comprehensive proteomic profiling of outer membrane vesicles from *Campylobacter jejuni*. *J. Proteomics* **98**, 90–98 (2014).
17. M. Gilbert, P. C. Godschalk, M. F. Karwaski, C. W. Ang, A. van Belkum, J. Li, W. W. Wakarchuk, H. P. Endtz, Evidence for acquisition of the lipooligosaccharide biosynthesis locus in *Campylobacter jejuni* GB11, a strain isolated from a patient with Guillain-Barré syndrome, by horizontal exchange. *Infect. Immun.* **72**, 1162–1165 (2004).
18. K. T. Young, L. M. Davis, V. J. Dirita, *Campylobacter jejuni*: Molecular biology and pathogenesis. *Nat. Rev. Microbiol.* **5**, 665–679 (2007).
19. I. Fonfara, A. Le Rhun, K. Chylinski, K. S. Makarova, A. L. Lécrivain, J. Bzdrenga, E. V. Koonin, E. Charpentier, Phylogeny of Cas9 determines functional exchangeability of dual-RNA and Cas9 among orthologous type II CRISPR-Cas systems. *Nucleic Acids Res.* **42**, 2577–2590 (2014).
20. M. Jinek, F. Jiang, D. W. Taylor, S. H. Sternberg, E. Kaya, E. Ma, C. Anders, M. Hauer, K. Zhou, S. Lin, M. Kaplan, A. T. Iavarone, E. Charpentier, E. Nogales, J. A. Doudna, Structures of Cas9 endonucleases reveal RNA-mediated conformational activation. *Science* **343**, 1247997 (2014).
21. F. Jiang, K. Zhou, L. Ma, S. Gressel, J. A. Doudna, A Cas9–guide RNA complex preorganized for target DNA recognition. *Science* **348**, 1477–1481 (2015).
22. E. C. LaCasse, Y. A. Lefebvre, Nuclear localization signals overlap DNA-or RNA-binding domains in nucleic acid-binding proteins. *Nucleic Acids Res.* **23**, 1647–1656 (1995).
23. M. K. Hibbard, R. M. Sandri-Goldin, Arginine-rich regions succeeding the nuclear localization region of the herpes simplex virus type 1 regulatory protein ICP27 are required for efficient nuclear localization and late gene expression. *J. Virol.* **69**, 4656–4667 (1995).
24. E. Haapaniemi, S. Botla, J. Persson, B. Schmierer, J. Taipale, CRISPR-Cas9 genome editing induces a p53-mediated DNA damage response. *Nat. Med.* **24**, 927–930 (2018).
25. R. J. Ihry, K. A. Worringer, M. R. Salick, E. Frias, D. Ho, K. Theriault, S. Kommineni, J. Chen, M. Sondey, C. Ye, R. Randhawa, T. Kulkarni, Z. Yang, G. McAllister, C. Russ, J. Reece-Hoyes, W. Forrester, G. R. Hoffman, R. Dolmetsch, A. Kaykas, P53 inhibits CRISPR-Cas9 engineering in human pluripotent stem cells. *Nat. Med.* **24**, 939–946 (2018).
26. S. Panier, S. J. Boulton, Double-strand break repair: 53BP1 comes into focus. *Nat. Rev. Mol. Cell Biol.* **15**, 7–18 (2014).
27. E. P. Rogakou, C. Boon, C. Redon, W. M. Bonner, Megabase chromatin domains involved in DNA double-strand breaks in vivo. *J. Cell Biol.* **146**, 905–916 (1999).
28. C. P. A. Skarp, O. Akinrinade, A. J. E. Nilsson, P. Ellström, S. Myllykangas, H. Rautelin, Comparative genomics and genome biology of invasive *Campylobacter jejuni*. *Sci. Rep.* **5**, 17300 (2015).
29. G. Iraola, R. Perez, H. Naya, F. Paolicchi, E. Pastor, S. Valenzuela, L. Calleros, A. Velilla, M. Hernández, C. Morsella, Genomic evidence for the emergence and evolution of pathogenicity and niche preferences in the genus *Campylobacter*. *Genome Biol. Evol.* **6**, 2392–2405 (2014).
30. M. Jinek, K. Chylinski, I. Fonfara, M. Hauer, J. A. Doudna, E. Charpentier, A programmable dual-RNA-guided DNA endonuclease in adaptive bacterial immunity. *Science* **337**, 816–821 (2012).
31. A. Elmi, E. Watson, P. Sandu, O. Gundogdu, D. C. Mills, N. F. Inglis, E. Manson, L. Imrie, M. Bajaj-Elliott, B. W. Wren, D. G. E. Smith, N. Dorrell, *Campylobacter jejuni* outer membrane vesicles play an important role in bacterial interactions with human intestinal epithelial cells. *Infect. Immun.* **80**, 4089–4098 (2012).
32. N. Crosetto, A. Mitra, M. J. Silva, M. Bienko, N. Dojer, Q. Wang, E. Karaca, R. Chiarle, M. Skrzypczak, K. Ginalski, P. Pasero, M. Rowicka, I. Dikic, Nucleotide-resolution DNA double-strand break mapping by next-generation sequencing. *Nat. Methods* **10**, 361–365 (2013).
33. M. Yamada, Y. Watanabe, J. S. Gootenberg, H. Hirano, F. A. Ran, T. Nakane, R. Ishitani, F. Zhang, H. Nishimasu, O. Nureki, Crystal structure of the minimal Cas9 from *Campylobacter jejuni* reveals the molecular diversity in the CRISPR-Cas9 systems. *Mol. Cell* **65**, 1109–1121.e3 (2017).
34. E. Kim, T. Koo, S. W. Park, D. Kim, K. Kim, H.-Y. Cho, D. W. Song, K. J. Lee, M. H. Jung, S. Kim, J. H. Kim, J. H. Kim, J.-S. Kim, *In vivo* genome editing with a small Cas9 orthologue derived from *Campylobacter jejuni*. *Nat. Commun.* **8**, 14500 (2017).
35. R. Sundaresan, H. P. Parameshwaran, S. D. Yogesha, M. W. Keilbarth, R. Rajan, RNA-independent DNA cleavage activities of Cas9 and Cas12a. *Cell Rep.* **21**, 3728–3739 (2017).
36. R. Louwen, A. Heikema, A. Van Belkum, A. Ott, M. Gilbert, W. Ang, H. P. Endtz, M. P. Bergman, E. E. Nieuwenhuis, The sialylated lipooligosaccharide outer core in *Campylobacter jejuni* is an important determinant for epithelial cell invasion. *Infect. Immun.* **76**, 4431–4438 (2008).
37. J. L. Aschner, M. Aschner, Nutritional aspects of manganese homeostasis. *Mol. Aspects Med.* **26**, 353–362 (2005).
38. D. Kerstan, G. A. Quamme, Intestinal absorption of magnesium, in *Calcium in Internal Medicine*, H. Morii, Y. Nishizawa, S. G. Massry, Eds. (Springer London, 2002), pp. 171–183.
39. J. T. McCarthy, R. Kumar, Divalent cation metabolism: Magnesium. *Atlas of Diseases of the Kidney* **1**, 1 (1999).
40. J. Lisher, D. Giedroc, Manganese acquisition and homeostasis at the host-pathogen interface. *Front. Cell. Infect. Microbiol.* **3**, 91 (2013).
41. J. A. Doudna, E. Charpentier, The new frontier of genome engineering with CRISPR-Cas9. *Science* **346**, 1258096 (2014).
42. P. Mali, L. Yang, K. M. Esvelt, J. Aach, M. Guell, J. E. DiCarlo, J. E. Norville, G. M. Church, RNA-guided human genome engineering via Cas9. *Science* **339**, 823–826 (2013).
43. E. Ma, L. B. Harrington, M. R. O'Connell, K. Zhou, J. A. Doudna, Single-stranded DNA cleavage by divergent CRISPR-Cas9 enzymes. *Mol. Cell* **60**, 398–407 (2015).
44. R. Louwen, E. E. S. Nieuwenhuis, L. van Marrewijk, D. Horst-Kreft, L. de Ruiter, A. P. Heikema, W. J. B. van Wamel, J. A. Wagenaar, H. P. Endtz, J. Samsom, P. van Baarlen, A. Akhmanov, A. van Belkum, *Campylobacter jejuni* translocation across intestinal epithelial cells is facilitated by ganglioside-like lipooligosaccharide structures. *Infect. Immun.* **80**, 3307–3318 (2012).

45. J. T. A. L. Hartjes, M. Vredenbregt-van den Berg, J. Veldhoven-Zweistra, C. Bangma; A. B. Houtsmuller; W. Weerden Van, G. W. Jenster, M. E. van Royen, in *ISEV2018 abstract book Journal of Extracellular Vesicles* (2018), pp. 14.
46. G. Dugar, S. L. Svensson, T. Bischler, S. Wäldchen, R. Reinhardt, M. Sauer, C. M. Sharma, The CsrA-FliW network controls polar localization of the dual-function flagellin mRNA in *Campylobacter jejuni*. *Nat. Commun.* **7**, 11667 (2016).
47. K. Tamura, G. Stecher, D. Peterson, A. Filipski, S. Kumar, MEGA6: Molecular evolutionary genetics analysis version 6.0. *Mol. Biol. Evol.* **30**, 2725–2729 (2013).
48. K. A. Talukder, M. Aslam, Z. Islam, I. J. Azmi, D. K. Dutta, S. Hossain, A. Nur-E-Kamal, G. B. Nair, A. Cravioto, D. A. Sack, H. P. Endtz, Prevalence of virulence genes and cytolethal distending toxin production in *Campylobacter jejuni* isolates from diarrheal patients in Bangladesh. *J. Clin. Microbiol.* **46**, 1485–1488 (2008).
49. J. Schindelin, I. Arganda-Carreras, E. Frise, V. Kaynig, M. Longair, T. Pietzsch, S. Preibisch, C. Rueden, S. Saalfeld, B. Schmid, J.-Y. Tinevez, D. J. White, V. Hartenstein, K. Eliceiri, P. Tomancak, A. Cardona, Fiji: An open-source platform for biological-image analysis. *Nat. Methods* **9**, 676–682 (2012).
50. P. Mohanraju, J. van der Oost, M. Jinek, D. C. Swarts, Heterologous expression and purification of CRISPR-Cas12a/Cpf1 protein. *Bio Protoc.* **8**, 10.21769/BioProtoc.2842, (2018).
51. É. Hegedüs, E. Kókai, A. Kotlyar, V. Dombrádi, G. Szabó, Separation of 1–23-kb complementary DNA strands by urea–agarose gel electrophoresis. *Nucleic Acids Res.* **37**, e112 (2009).
52. R. O. Watson, J. E. Galán, *Campylobacter jejuni* survives within epithelial cells by avoiding delivery to lysosomes. *PLOS Pathog.* **4**, e14 (2008).

Acknowledgments: We would like to acknowledge the contributions of A. Akhmanova, J. Doudna, T. Mahmoudi, and M. Mubashir Khalid for providing plasmids and/or antibodies. We would like to thank C. M. Sharma and D. S. Weiss for helpful discussions. **Funding:** C.S. is a graduate student at Erasmus Postgraduate School of Molecular Medicine and is partially supported by I&I Fund (Erasmus Vrienden Fonds) and LSH-TKI foundation grant LSHM18006. S.B. is supported by the Ride for the Roses Cancer Research Grant obtained from the Dutch Cancer Society. J.v.d.O. is financially supported by the Netherlands Organization of Scientific Research (NWO, TOP grant 714.015.001) and R.L. by the Department of Medical Microbiology and Infectious Diseases and the Department of Bioinformatics, Erasmus MC. C.L. and J.H.G.L. are supported by the Oncode Institute, which is partly financed by the Dutch Cancer Society (KWF) and the Dutch Research Council (NWO). The bioinformatics team of P.J.v.d.S. receives supporting funding from H2020 projects ImmuneAID and Moodstratification for Data analysis infrastructure. Moreover, National funding has been obtained from the ZonMW project Genomes First for genomics infrastructure. **Author contributions:** C.S., P.M., G.-J.K., J.H.G.L., D.v.G., J.W.M., P.v.B., J.v.d.O., P.J.v.d.S., and R.L. contributed to the conception and design of the project. C.S., P.M., G.D., G.-J.K., W.A.v.C., D.H.-K., C.L. S.B., D.G., D.B., M.K., R.J., and R.L. performed the experiments and analyzed the data. A.S. and Y.H. performed the sequencing analysis. J.H.G.L., D.v.G., J.W.M., P.J.v.d.S., J.v.d.O., and R.L. edited the manuscript. C.S., P.M., P.v.B., J.v.d.O., and R.L. wrote the manuscript, which was read and approved by all authors. **Competing interests:** A related patent application have been filed under number WO2017155408A1. All authors declare that they have no competing interests. **Data and materials availability:** Sequencing data are available at European Nucleotide Archive under accession number PRJEB34300. The generated genetic modified organisms and plasmids can be provided by the Erasmus MC pending scientific review and a completed material transfer agreement. Requests for the genetic modified organisms and plasmids should be submitted to R.L. (r.louwen@erasmusmc.nl). All data needed to evaluate the conclusions in the paper are present in the paper and/or the Supplementary Materials. Additional data related to this paper may be requested from the authors.

Submitted 12 September 2019
Accepted 6 May 2020
Published 17 June 2020
10.1126/sciadv.aaz4849

Citation: C. Saha, P. Mohanraju, A. Stubbs, G. Dugar, Y. Hoogstrate, G.-J. Kremers, W. A. van Cappellen, D. Horst-Kreft, C. Laffeber, J. H. Lebbink, S. Bruens, D. Gaskin, D. Beerens, M. Klunder, R. Joosten, J. A. A. Demmers, D. van Gent, J. W. Mouton, P. J. van der Spek, J. van der Oost, P. van Baarlen, R. Louwen, Guide-free Cas9 from pathogenic *Campylobacter jejuni* bacteria causes severe damage to DNA. *Sci. Adv.* **6**, eaaz4849 (2020).

ScienceAdvances

Guide-free Cas9 from pathogenic *Campylobacter jejuni* bacteria causes severe damage to DNA

Chinmoy Saha, Prarthana Mohanraju, Andrew Stubbs, Gaurav Dugar, Youri Hoogstrate, Gert-Jan Kremers, Wiggert A. van Cappellen, Deborah Horst-Kreft, Charlie Laffeber, Joyce H.G. Lebbink, Serena Bruens, Duncan Gaskin, Dior Beerens, Maarten Klunder, Rob Joosten, Jeroen A. A. Demmers, Dik van Gent, Johan W. Mouton, Peter J. van der Spek, John van der Oost, Peter van Baarlen and Rogier Louwen

Sci Adv **6** (25), eaaz4849.
DOI: 10.1126/sciadv.aaz4849

Science Advances (ISSN 2375-2548) is published by the American Association for the Advancement of Science, 1200 New York Avenue NW, Washington, DC 20005. The title *Science Advances* is a registered trademark of AAAS.